Toxicology Reports 1 (2014) 341–352

Contents lists available at ScienceDirect

Toxicology Reports

journal homepage: www.elsevier.com/locate/toxrep

Cytotoxicity and enzyme inhibition studies of polyoxometalates and their chitosan nanoassemblies

Hamid Saeed Shah[a], Rami Al-Oweini[b], Ali Haider[b], Ulrich Kortz[b], Jamshed Iqbal[a,*]

[a] Centre for Advanced Drug Research, COMSATS Institute of Information Technology, Abbottabad 22060, Pakistan
[b] School of Engineering and Science, Jacobs University, P.O. Box 750 561, 28725 Bremen, Germany

ARTICLE INFO

Article history:
Received 29 March 2014
Received in revised form 1 June 2014
Accepted 1 June 2014
Available online 6 June 2014

Keywords:
Polyoxometalate
Chitosan
Cytotoxicity
Alkaline phosphatase
Chitosan-polyoxometalate nanoassemblies

ABSTRACT

Polyoxometalates (POMs) have become very significant in biomedical research for their structural diversity which renders them highly active against bacterial, viral and cancer diseases. In this study three different POMs were synthesized and nanoassemblies were made with chitosan (CTS), a natural biodegradable polymer with excellent drug carrier properties. The compounds were tested on two isoenzymes of alkaline phosphatases including tissue specific calf intestine alkaline phosphatase (CIAP) and tissue non-specific alkaline phosphatase (TNAP). Compound $[TeW_6O_{24}]^{6-}$ (TeW_6) showed the highest activity (45.4 ± 11.3 nM) among tested compounds against TNAP. Similarly, chitosan-$[TeW_6O_{24}]^{6-}$ (CTS-TeW_6) was proved to be a potent inhibitor of CIAP with K_i value of 22 ± 7 nM. A comparative study was made to evaluate their cytotoxic potential against HeLa cells. Among all tested compounds, Chitosan-$[NaP_5W_{30}O_{110}]^{14-}$ (CTS-P_5W_{30}) has showed higher percent cytotoxicity ($88 \pm 10\%$) at 10 μM when compared with the standard anticancer drug vincristine ($72 \pm 7\%$). The study revealed that selected POMs proved excellent anticancer potential and were equally effective against alkaline phosphatase enzyme, an increased level of which may indicate cancer metastasis.

1. Introduction

Polyoxometalates (POMs) are discrete metal oxide clusters of early transition metal ions in high oxidation states (*e.g.* W^{6+}, Mo^{6+}, V^{5+}), which exhibit exceptional diversity in shape, size, and structural properties [1–4]. POMs are classified in two distinct families, namely, iso- and heteropolyanions [5,6]. The number of heteropolyanions is larger than that of isopolyanions, thus making them highly interesting compounds for several applications and fields of study. Such attributes, in addition to their solubility and stability at physiological pH, render them very attractive in medicine [6–10]. Another promising feature of POMs is that they can easily interact and bind to the target macromolecule because of their diversity in size, shape, polarity, surface charge distribution, and redox potential which improves their bonding properties [11].

Bioinorganic metal complexes have been studied extensively for targeted anticancer drug therapy [12–15]. The most promising metal-based anticancer drug is cisplatin, which is effective against lymphomas, head, neck, bladder and ovarian cancers [16–18]. POMs have excellent potential to treat various types of cancers including pancreatic cancer [19], leukemia [20], hepatocellular carcinoma [21], colon carcinoma [22], ovarian cancer [23], gastric cancer [24], among others. Moreover, POMs were reported to

* Corresponding author. Tel.: +92 992 383591 96; fax: +92 992 383441.
E-mail addresses: drjamshed@ciit.net.pk, jamshediqb@gmail.com, jamshed.iqbal@uni-bonn.de (J. Iqbal).

http://dx.doi.org/10.1016/j.toxrep.2014.06.001

stimulate insulin secretion and regenerate pancreatic beta cell function in rodents [25–31]. POMs are also very effective in treating bacterial [32–34] and viral [35–38] diseases. A very recent study shows the ability of POMs, specifically $[TeW_6O_{24}]^{6-}$, to act as a co-crystallization agent in the isolation and crystallization of the latent isoform PPO4 mushroom (*Agaricus bisporus*) tyrosinase protein which helps in the catalytic activity of phenols oxidation to quinones which in turn are responsible for the generation of melanins by polymerization [39].

Encapsulation of POMs into a biodegradable polymer has been studied previously, which enhances its stability at physiological pH, hence improving antiviral, antibacterial and anticancer properties [33,40–43]. Chitosan (CTS) is a natural, biodegradable polymer that has become one of the most widely studied biomaterial so far. Chitosan is obtained by de-acetylation of chitin, an essential polysaccharide, which is found in the exoskeleton of shrimps and crab shells [44,45]. Chitosan can be effectively used in extended release drug delivery system because it is degraded in the human body by ubiquitous enzymes chitosanase and lysozyme which aid in releasing the drug in a controlled and precise manner [46,47]. A combination of chitosan with inorganic, bioactive compounds suggests high potential for the development of new drug molecules with low toxicity, high stability and effective bio-distribution [48–52].

Ectonucleotidases represent a membrane-bound enzymes family, which mainly includes ecto-nucleoside triphosphate diphosphohydrolases (E-NTPDases) and alkaline phosphatases that are involved in nucleotide metabolism. Inhibition of these enzymes may increase the immune response and helps in combating cancer, auto-immune diseases as well as bacterial and viral infections [53]. POMs have been identified as potent and selective inhibitors of NTPDases [54] and alkaline phosphatases [55,56]. Alkaline phosphatase level usually rises in colon, breast, lung, thyroid and prostate cancer when it metastasizes to bone and liver [57–62].

In the present study, POMs and their respective CTS associated nanoassemblies were synthesized, structurally characterized and evaluated for inhibition activity against alkaline phosphatase isoenzymes (TNAP and CIAP). In addition, a comparative *in vitro* cytotoxicity analysis of synthesized compounds with standard anticancer drug vincristine (VCN) was carried out on human cervical adenocarcinoma (HeLa) cells.

2. Materials and methods

All chemicals used for the synthesis of the POMs were purchased commercially and used as received without further purification. Chitosan (YC-100) (M ~10,000 g/mol), tissue non-specific alkaline phosphatase enzyme (TNAP), L-phenylalanine, levamisole, Tris–HCl, Tris base, $MgCl_2$, $ZnCl_2$, RPMI-1640, fetal bovine serum (FBS), penicillin and streptomycin were purchased from Sigma–Aldrich, Steinheim, Germany. Tissue specific alkaline phosphatase enzyme extracted from calf intestine (CIAP) was obtained from Calbiochem, Germany. Human cervical adenocarcinoma cell line (HeLa) was purchased from ATCC (ATCC CRL-5802) and vero cell line was acquired from RIKEN Bio Resource Center, Japan.

POMs were synthesized and encapsulated with CTS to form CTS-POMs nanoassemblies. The synthesis and characterization of these materials are given below.

2.1. Synthesis of $(NH_4)_{14}[NaP_5W_{30}O_{110}]\cdot 31H_2O$

$(NH_4)_{14}[NaP_5W_{30}O_{110}]\cdot 31H_2O$ (NH_4-P_5W_{30}) was synthesized according to a previously described method [63], and characterized by FT-IR (Fig. 3b) and ^{31}P NMR spectroscopy. ^{31}P NMR spectrum (Fig. 2a) obtained shows the characteristic signal at −9.4 ppm The structure of the polyanion is shown in Fig. 1a.

2.2. Synthesis of chitosan-$[NaP_5W_{30}O_{110}]^{14-}$ nanoassembly

Chitosan-$[NaP_5W_{30}O_{110}]^{14-}$ (CTS-P_5W_{30}) nanoassembly was synthesized by dissolving 0.50 g (0.71 mM) of chitosan (CTS) in 70 mL of distilled water. The resultant solution was filtered (solution I). Similarly, 1.24 g (21.38 mM) of $[NaP_5W_{30}O_{110}]^{14-}$ was dissolved in 30 mL of H_2O and the obtained solution was filtered (solution II). Solution II was added dropwise to solution I, and then gel-like precipitates were formed and separated from the solution by means of filtration, washed and air-dried. The obtained product was characterized by FT-IR spectroscopy (Fig. 3a), where the appearance of 936, 910, 795,

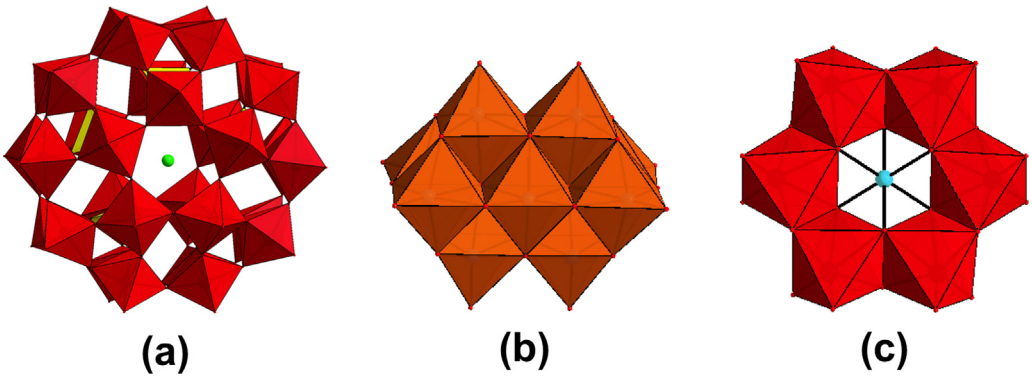

Fig. 1. Structural representations of the POMs. (a) $[NaP_5W_{30}O_{110}]^{14-}$ (P_5W_{30}), (b) $[V_{10}O_{28}]^{6-}$ (V_{10}), (c) $[TeW_6O_{24}]^{6-}$ (TeW_6).

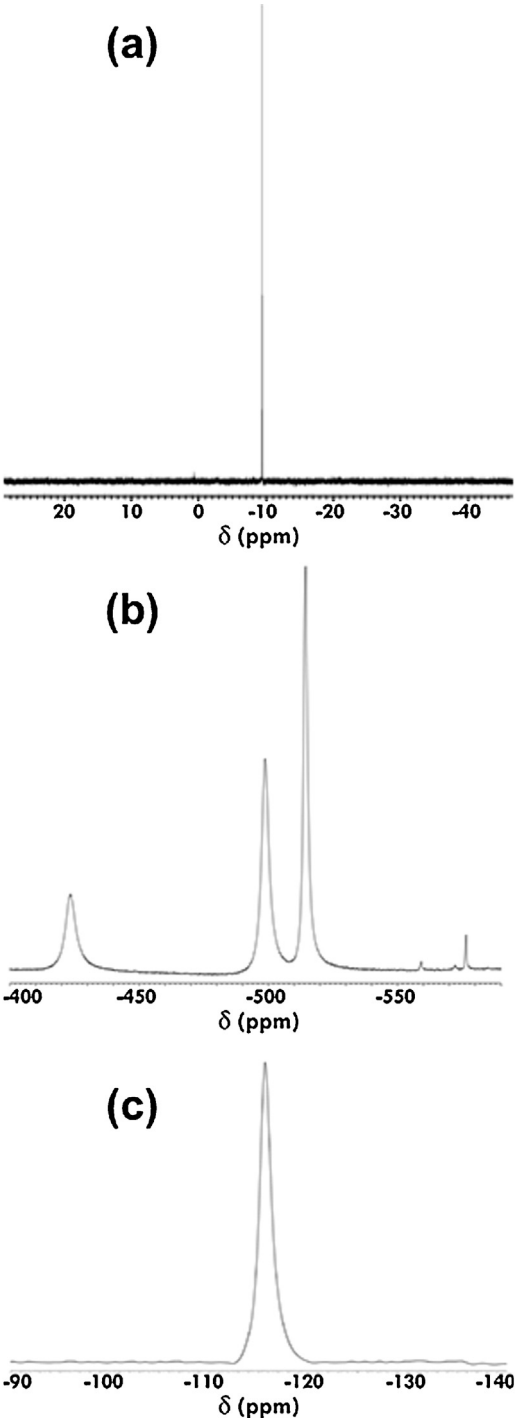

Fig. 2. A representative NMR spectra of POMs. (a) ^{31}P NMR spectrum of $(NH_4)_{14}[NaP_5W_{30}O_{110}]\cdot 31H_2O$ ($(NH_4)_{14}$-P_5W_{30}) in H_2O/D_2O ($\delta = -9.4$ ppm); (b) ^{51}V NMR spectrum of $Na_6[V_{10}O_{28}]\cdot 18H_2O$ (Na_6-V_{10}) in H_2O/D_2O ($\delta = -423.3$ V_{10A}, -498.8 V_{10B}, -514.4 V_{10C} and -576.5 V_1 ppm); (c) ^{183}W NMR spectrum of $Na_6[TeW_6O_{24}]\cdot 22H_2O$ (Na_6-TeW_6) in H_2O/D_2O ($\delta = -115.6$ ppm).

737 and 570 cm^{-1} bands confirmed the formation of the nanoassembly.

2.3. Synthesis of $Na_6[V_{10}O_{28}]\cdot 18H_2O$

Compound $Na_6V_{10}O_{28}\cdot 16H_2O$ (Na_6-V_{10}) (Fig. 1b) was prepared by adapting previously described methods [64,65]. Typically, $NaVO_3$ (3 g, 24.6 mmol) is dissolved in 100 mL water and HCl (4 M) was used to reduce the pH to 4.8. The solution was filtered and HCl was added to maintain the pH at 4.5. The bulk sodium salt of the polyanion was obtained by the addition of 200 mL ethanol (95%, v/v), leading to an orange color precipitates, which were removed by filtration and air-dried. The product was characterized by FT-IR (Fig. 4b) and ^{51}V NMR spectroscopy, where V_1 corresponds to the monomeric (VO_4^{3-}) vanadate species whereas V_{10A}, V_{10B} and V_{10C} signals correspond to the V(3), V(1) and V(2) vanadium atoms in the decameric vanadate species ($V_{10}O_{28}^{6-}$). ^{51}V NMR spectrum obtained (Fig. 2b) shows the characteristic signal of decameric (V10A at -423.3 ppm; V_{10B} at -498.8 ppm; V_{10C} at -514.4 ppm) and monomeric species (V1 at -576.5 ppm). The structure of polyanion is shown in Fig. 1b.

2.4. Synthesis of chitosan-$[V_{10}O_{28}]^{6-}$ nanoassembly

Synthesis of the chitosan-$[V_{10}O_{28}]^{6-}$ (CTS-V_{10}) nanoassembly was carried out by dissolving 0.50 g (0.71 mM) of chitosan (CTS) in 70 mL of distilled water and filtered (solution I). A 0.43 g (10.1 mM) of $[V_{10}O_{28}]^{6-}$ was dissolved in 30 mL of distilled water and filtered (solution II). The solution (II) was added dropwise to solution (I). The gel-like precipitates were formed and separated from the solution by means of filtration, washed and air-dried. The obtained product was characterized by FT-IR spectroscopy (see Fig. 4a), where the appearance of 1074, 950, 821, and 744 cm^{-1} bands confirmed the formation of the nanoassembly.

2.5. Synthesis of $Na_6[TeW_6O_{24}]\cdot 22H_2O$

$Na_6[TeW_6O_{24}]\cdot 22H_2O$ (Na_6-TeW_6) (Fig. 1c) was synthesized by previously reported method with some modifications [66] Briefly, A mixture of $Na_2WO_4\cdot 2H_2O$ (5.0 g, 15.2 mmol) and $Te(OH)_6$ (0.6 g, 2.6 mmol) were dissolved in 100 mL of water. The pH was adjusted to 5.0 with HCl (1 M) followed by heating at 110 °C until about one fourth of the solvent has been evaporated. The solution was allowed to cool and filtered. Slow evaporation of the filtrate at room temperature for one week led to the formation of colorless crystals, which were collected by filtration and air-dried. The product was characterized by FT-IR (Fig. 5b) and ^{183}W NMR spectroscopy. ^{183}W NMR spectrum obtained (Fig. 2c) shows the characteristic signal at 115.6 ppm. The structure of polyanion is shown in Fig. 1c.

2.6. Synthesis of chitosan-$[TeW_6O_{24}]^{6-}$ nanoassembly

Chitosan-$[TeW_6O_{24}]^{6-}$ (CTS-TeW_6) nanoassembly was synthesized by dissolving 0.50 g (0.71 mM) of CTS in 70 mL

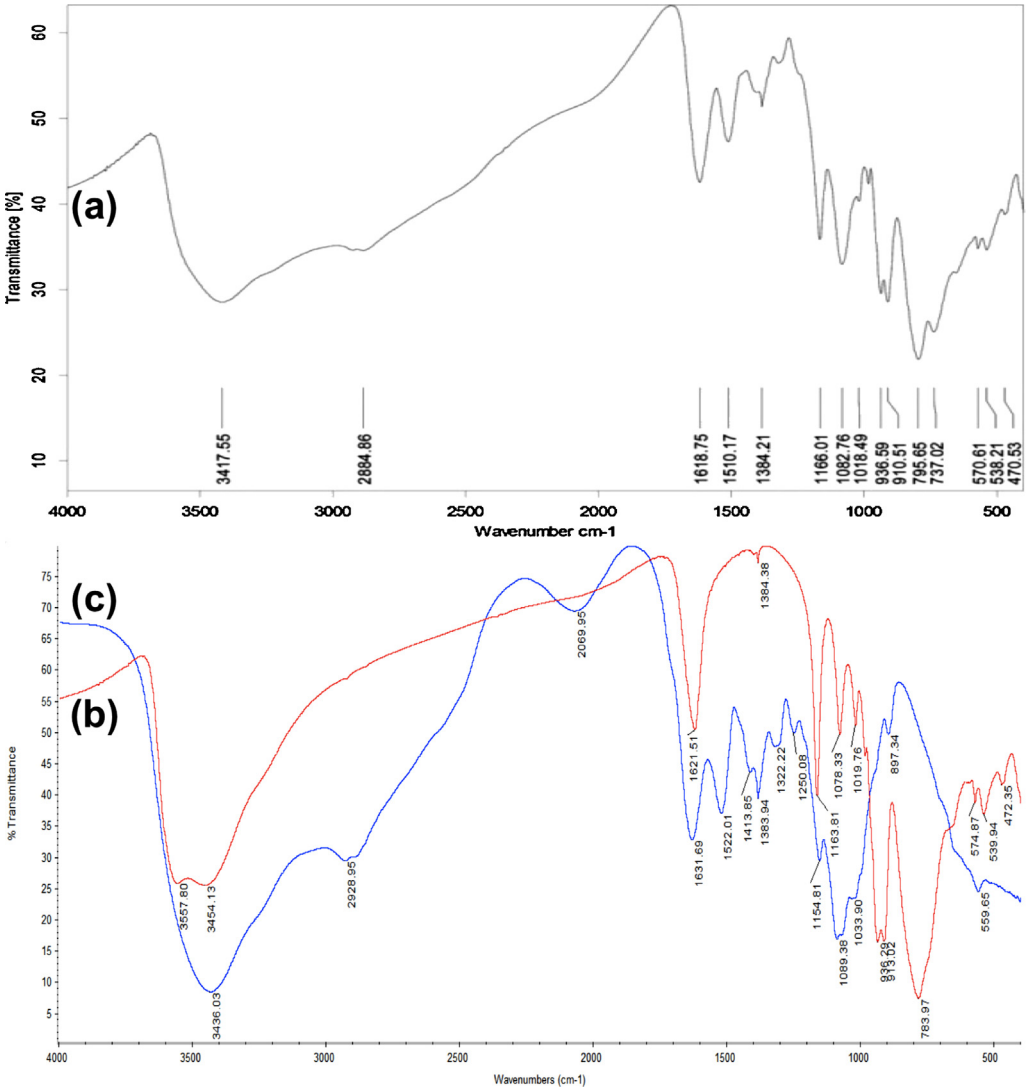

Fig. 3. The FT-IR spectra of (a) CTS-P_5W_{30}, (b) P_5W_{30} (red line), and (c) CTS (blue line). (For interpretation of the references to color in this figure legend, the reader is referred to the web version of the article.)

distilled water. The resultant solution was filtered (solution I). Similarly, 0.64 g (9.9 mM) of $[TeW_6O_{24}]^{6-}$ was dissolved in 30 mL H_2O and the product was filtered (solution II). Solution (II) was added dropwise into solution (I) leading to the formation of gel-like precipitates which were separated by filtration and washed several times with water and air-dried. The obtained product was characterized by FT-IR spectroscopy (Fig. 5a), where the appearance of 948, 903, 679, 617 and 556 cm^{-1} bands confirmed the formation of the nanoassembly.

2.7. Zeta potential and particle size measurement

The CTS-POMs nanoassemblies were characterized by zeta potential to check their stability in colloidal suspension. Furthermore the particle size of the selected compound CTS-P_5W_{30} was also determined.

2.8. Enzyme inhibition studies against alkaline phosphatases

Each compound was tested on TNAP and CIAP enzymes. Each enzyme was diluted in a buffer having pH 9.5 prepared from 50 mM Tris–HCl, 5 mM $MgCl_2$, 0.1 mM $ZnCl_2$ and 50% glycerol. A 0.5 mM enzyme substrate *p*-nitrophenyl phosphate (*p*-NPP) solution was also prepared in assay buffer (pH 9.5) comprised of 50 mM Tris–HCl, 5 mM $MgCl_2$, 0.1 mM $ZnCl_2$ without glycerol.

The initial screening of test compounds was done at 0.1 mM concentration by using a previously described spectrophotometric method [67]. The standard inhibitors were employed for initial screening to compare and evaluate the inhibition capacity of test compounds. Levamisole was used as standard inhibitor of TNAP [68] while L-phenylalanine was used for CIAP [69]. Briefly, the compounds which showed ≥50% inhibition were selected and

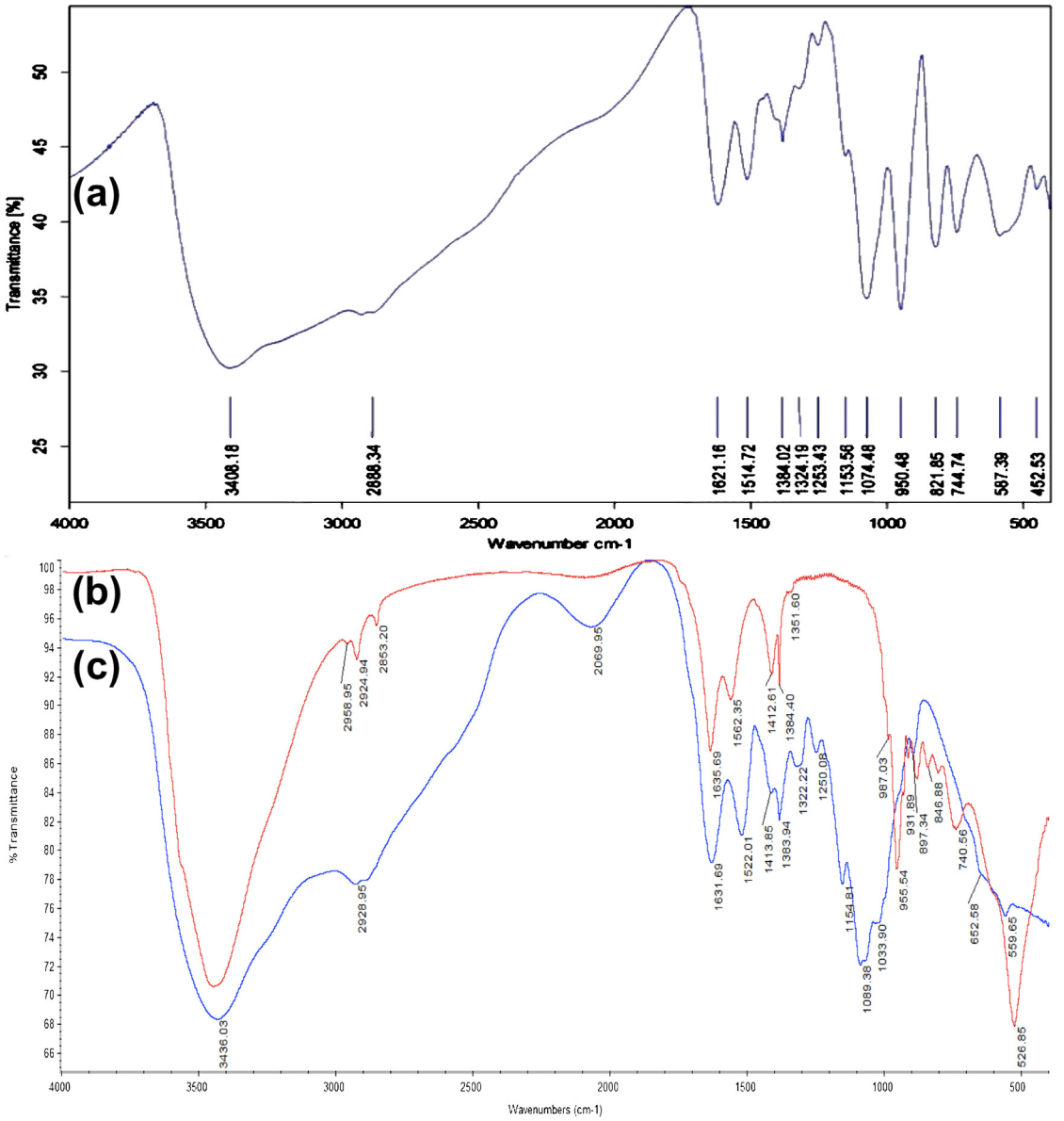

Fig. 4. The FT-IR spectra of (a) CTS-V_{10}, (b) V_{10} (red line), and (c) CTS (blue line). (For interpretation of the references to color in this figure legend, the reader is referred to the web version of the article.)

further tested to determine dose–response curve of each inhibitor. Generally, each compound was pre-incubated with 10 μL of enzyme and 70 μL of assay buffer at 37 °C for 10 min A 10 μL of *p*-NPP was added and the mixture was again incubated for 30 minutes The product (*p*-nitrophenolate) formed was measured on ELISA plate reader (Bio-TekELx 800^{TM}, Instruments, Inc. USA) at wavelength of 405 nm. The experiments were done in triplicate. The respective K_i value of each inhibitor was calculated by using Prism 5.0 (GraphPad Software, San Diego, CA, USA).

2.9. Cell lines and cell cultures

HeLa cells and vero cells were cultured in a medium containing RPMI-1640 supplemented with L-glutamine (2 mM), penicillin (100 U mL^{-1}) and streptomycin (100 μg mL^{-1}) accompanied with 10% FBS and stored in an incubator supplied with 5% CO_2 at a constant temperature of 37 °C. When both adherent cell lines were confluent the cells were cultivated in 96-well plates at a seeding density of 10^4 cells in 100 μL to conduct cytotoxicity assays.

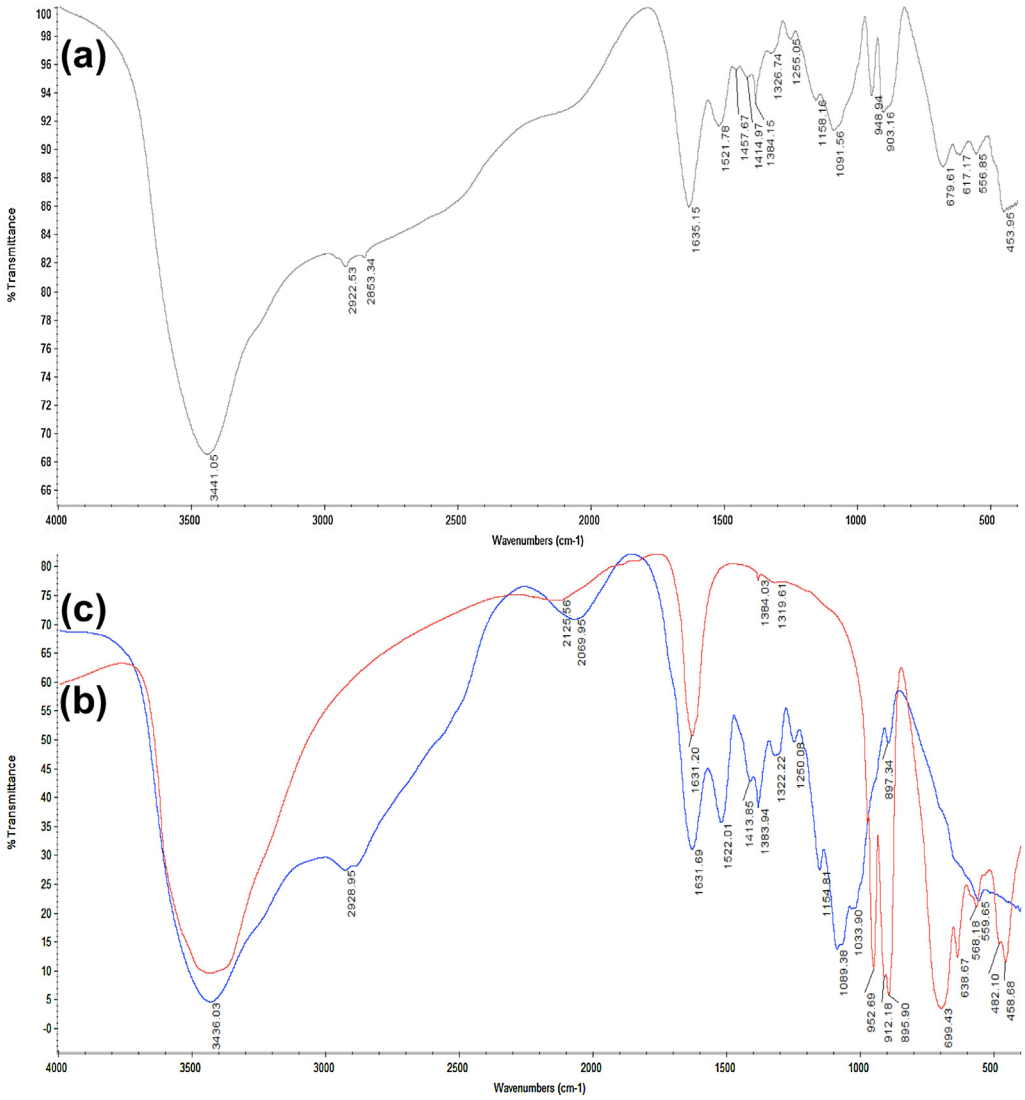

Fig. 5. The FT-IR spectra of (a) CTS-TeW_6, (b) TeW_6 (red line), and (c) CTS (blue line). (For interpretation of the references to color in this figure legend, the reader is referred to the web version of the article.)

2.10. Cytotoxicity analysis by sulforhodamine B (SRB) assay

A previously described colorimetric cytotoxicity assay was adopted which measures cellular protein content of cells [70]. Concisely, Hela cells and vero cells were seeded in 96 well plates for 24 h. Different concentrations of test compounds (10, 1, 0.1 μM) were made and inoculated in test wells of 96 well plates and incubated for up to 48 h. Likewise, the control and blank wells were also prepared containing VCN and culture medium respectively. After incubation, the cells were fixed with 50 μL of 50% ice cold TCA solution for 1 h. The plates were washed 5 times with PBS and air dried. The fixed cells were further treated with 0.4% (w/v) sulforhodamine B dye prepared in 1% acetic acid solution and left at room temperature for 30 min The plates were rinsed with 1% acetic acid solution and allowed to dry. In order to solubilize the dye, a 10 mM Tris base solution was added and left for 10 min at room temperature. The absorbance was measured at 490 nm subtracting the background measurement at 630 nm.

3. Results and discussion

3.1. Synthesis of POMs and their chitosan based nanoassemblies

POMs and their chitosan linked nanoassemblies were synthesized and characterized by NMR, and FT-IR. The results are presented in Figs. 1–5.

3.2. Characterization of chitosan-POMs nanoassemblies

The successful formations of chitosan-POM nanoassemblies were confirmed by the appearance of characteristic bands in the region of 1000–500 cm^{-1} in the respective

Table 1
Zeta potential measurement of POMs and their chitosan nanoassemblies.

Code	Particle size ± SEM[a] (nm)	Zeta potential ± SEM[a] (mV)
CTS-P_5W_{30}	100	−44.56 ± 2.48
CTS-V_{10}	–	−23.83 ± 1.09
CTS-TeW_6	–	−37.06 ± 2.55

[a] SEM of 3 experiments performed in triplicate.

FT-IR spectra as compare to that of simple POM FT-IR spectra. The stability of chitosan-POM nanoassemblies was determined by zeta potential measurement which was found in the range of −23 to −45 mV (see Table 1). The maximum stability was given by CTS-P_5W_{30} with zeta potential of −44.56 ± 2.48 mV (see Fig. 6b) while particle size of CTS-P_5W_{30} was also determined with transmission electron microscopy (TEM) that was 100 nM (see Fig. 6a). A possible reason for negative zeta potential is the presence of a highly negative charge on the polyanions [71].

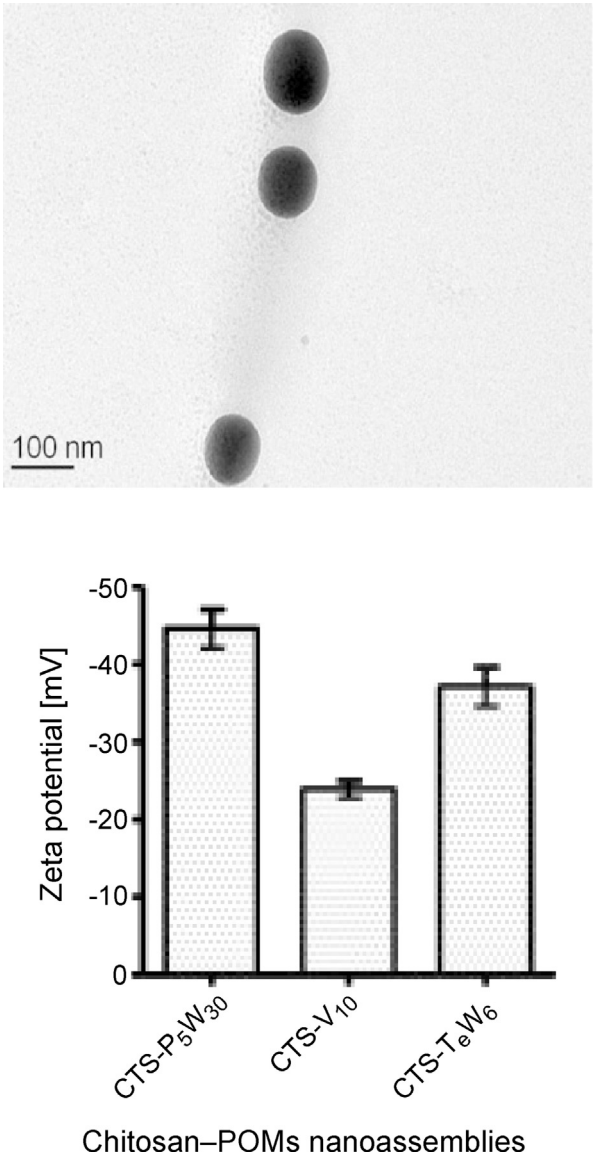

Fig. 6. A representation of particle size measurement and zeta potential of CTS-POMs, (a) TEM image of CTS-P_5W_{30} (b) zeta potential measurement of CTS-POMs nanoassemblies.

3.3. Inhibition studies on alkaline phosphatases

An elevated level of the alkaline phosphatase enzyme has been studied as a non-specific tumor marker associated with certain abnormalities in physiological functions of human body [72,73]. In recent years, the biological significance of POMs has become apparent and many studies have been reported in this context [21,54,74]. The present study was presented on the synthesis and evaluation of POMs and their CTS associated nanoassemblies, which were found potent inhibitor of alkaline phosphatases with K_i values in nano molar range

POMs and CTS-POMs nanoassemblies were tested against two different isoenzymes of alkaline phosphatase, *i.e.* CIAP and TNAP. The test compounds were initially screened at 0.1 mM end concentration, which showed more than 70% inhibition on both isoenzymes. In order to find K_i value, a 3-fold serial dilution of each compound was made and K_i value was determined in nano molar range. Among CTS-POMs nanoassemblies the highest inhibition against CIAP was given by CTS-TeW_6, with a K_i value of 22 ± 7 nM, while CTS-P_5W_{30} and CTS-V_{10} also showed a decent inhibition with 31.1 ± 7.8 nM and 509 ± 17 nM, respectively. The TeW_6 was the most potent TNAP inhibitor among all tested compounds with a K_i value of 45.4 ± 11.3 nM. A possible reason for higher selectivity and inhibition potential of CTS-TeW_6 and TeW_6 may be due to the presence of tellurium metal, which has been proved previously in reducing ALP levels in diabetic rats [75]. Dose–response curves of were made (Fig. 7) and presented in a comparative manner to evaluate the activity against ALP isoenzymes (see Table 2).

3.4. Anticancer activity studies

3.4.1. Cytotoxicity assay

POMs and their chitosan-encapsulated nanoassemblies were tested as anticancer agents on HeLa cells. The test compounds were prepared in different concentration ranges of 10, 1 and 0.1 μM. All test compounds showed good cytotoxicity against HeLa cells, even at the lowest concentration of 0.1 μM with minimum toxicity against vero cells (see Table 3). The maximum cytotoxicity against HeLa cells was observed with the compound CTS-P_5W_{30} having percent inhibition of 88 ± 10 (see Fig. 8), that may be due to the higher number of phosphorous (P) and tungsten (W) atoms [55].

A difference of cytotoxicity behavior was observed between P_5W_{30}, TeW_6, CTS-P_5W_{30} and CTS-TeW_6, which support the idea that the encapsulation of POMs into a biopolymer may render polyanion more target oriented, with minimal adverse effects [76]. The vanadium (V) containing compounds have previously been reported as good anticancer and antidiabetic agents [77,78]. Here we have synthesized compounds V_{10} and CTS-V_{10} which also showed promising cytotoxicity behavior 66 ± 15% and 81 ± 9% respectively. The compound CTS-TeW_6 has

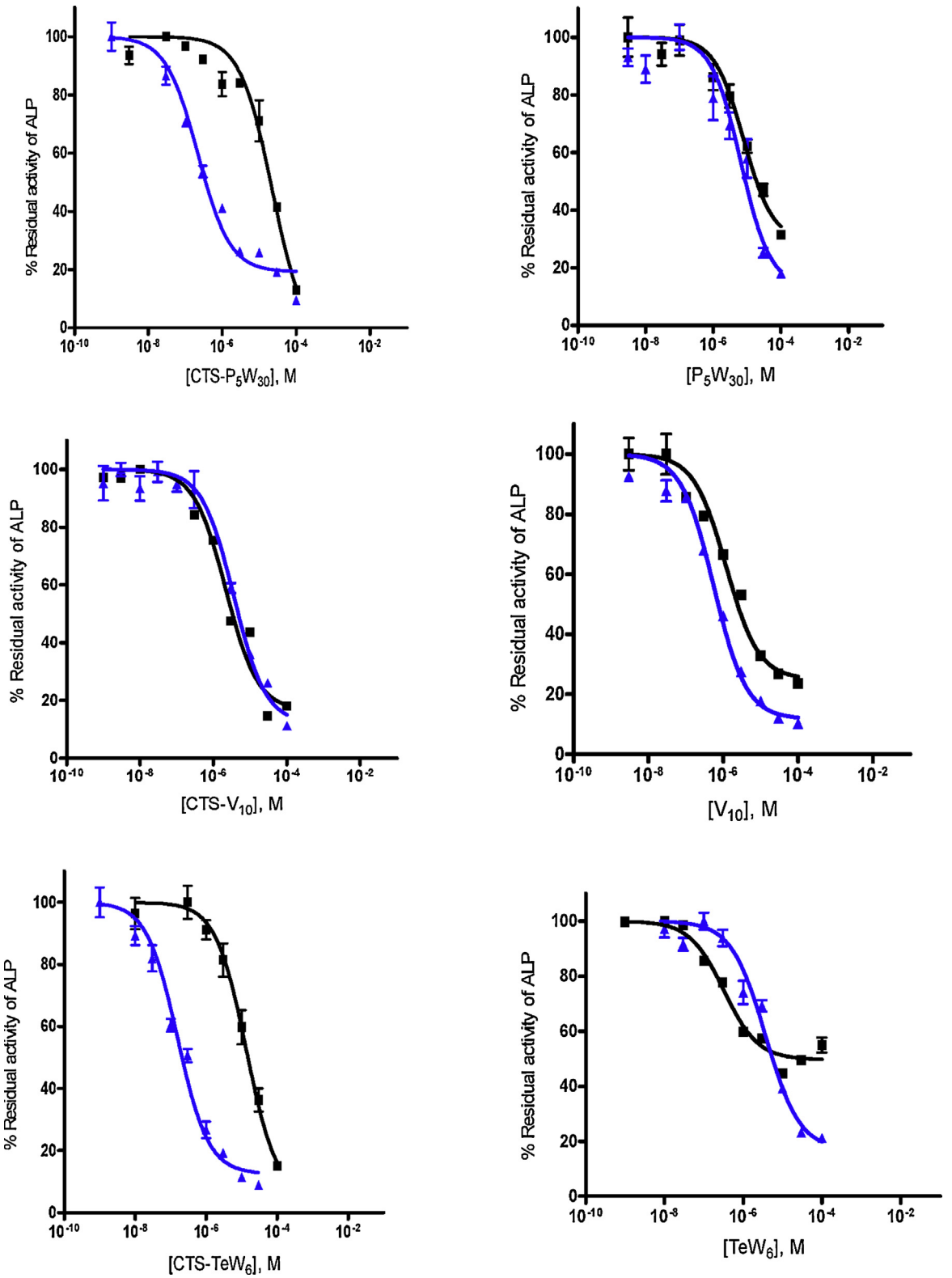

Fig. 7. The potential activities of POMs and their chitosan based nanoassemblies on CIAP (blue line) and TNAP (black line) isoenzymes. (For interpretation of the references to color in this figure legend, the reader is referred to the web version of the article.)

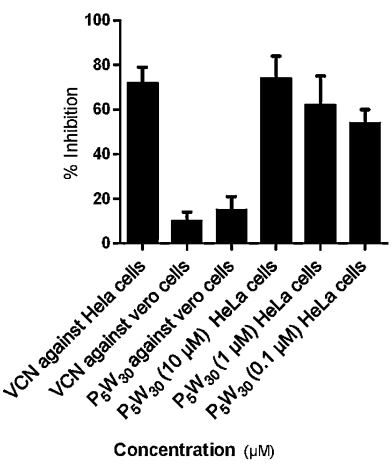

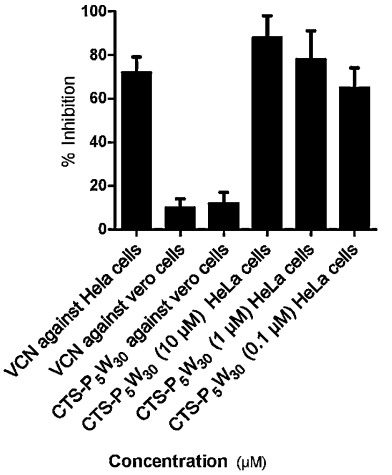

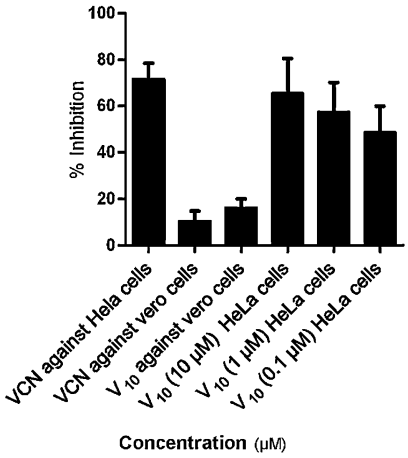

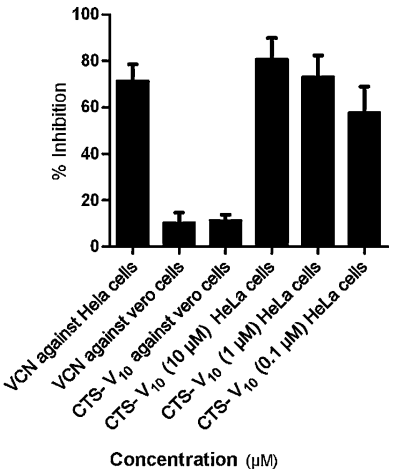

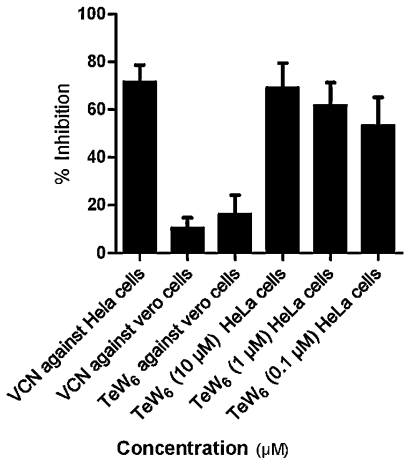

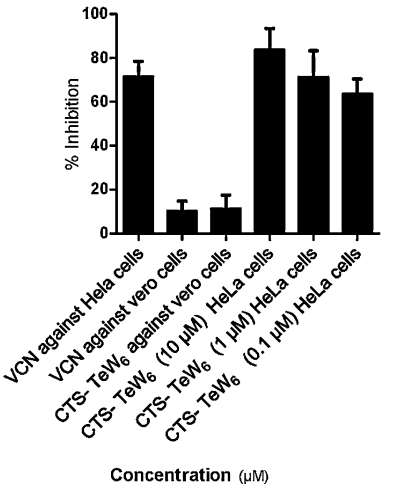

Fig. 8. A graphical representation of multiple comparisons of anticancer activities between POMs, their chitosan based nanoassemblies and VCN.

Table 2
Activities of POMs and CTS based nanoassemblies against CIAP and TNAP.

No.	Code	Molecular formula/structure	K_i (nM) ± SEM[a]	
			CIAP[b]	TNAP[c]
1	P_5W_{30}	$(NH_4)_{14}[NaP_5W_{30}O_{110}]\cdot 31H_2O$	921 ± 6	1112 ± 36
2	CTS-P_5W_{30}	Chitosan-$[NaP_5W_{30}O_{110}]^{14-}$	31.1 ± 7.8	3179 ± 84
3	V_{10}	$Na_6[V_{10}O_{28}]\cdot 18H_2O$	79.1 ± 2.3	169 ± 21
4	CTS-V_{10}	Chitosan-$[V_{10}O_{28}]^{6-}$	509 ± 17	308 ± 63
5	TeW_6	$Na_6[TeW_6O_{24}]\cdot 22H_2O$	520 ± 13	45.4 ± 11.3
6	CTS-TeW_6	Chitosan-$[TeW_6O_{24}]^{6-}$	22 ± 7	1921 ± 54
7	L-phenylalanine	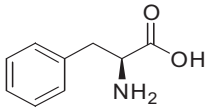	75%	–
8	Levamisole	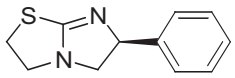	–	71%

[a] SEM = standard error of mean of 3 experiments.
[b] CIAP (calf intestinal alkaline phosphatase).
[c] TNAP (tissue non-specific alkaline phosphatase).

Table 3
The cytotoxicity comparison of vincristine, POMs and their chitosan based nanoassemblies on Hela and vero cells.

Codes	Percent inhibition ± SEM[a] at 10 μM on vero cells	Percent inhibition ± SEM at 10 μM on Hela cells	Percent inhibition ± SEM at 1 μM on Hela cells	Percent inhibition ± SEM at 0.1 μM on Hela cells
VCN[b]	10 ± 4	72 ± 7	–	–
P_5W_{30}	15 ± 6	74 ± 10	62 ± 13	54 ± 6
CTS-P_5W_{30}	12 ± 5	88 ± 10	78 ± 15	65 ± 9
V_{10}	16 ± 3	66 ± 15	57 ± 13	49 ± 11
CTS-V_{10}	11 ± 2	81 ± 9	73 ± 9	58 ± 11
TeW_6	16 ± 8	69 ± 10	62 ± 10	53 ± 12
CTS-TeW_6	11 ± 6	84 ± 10	71 ± 12	64 ± 7

[a] SEM Standard error of mean of 3 experiments performed in triplicate.
[b] VCN (vincristine).

anticancer activity of 84 ± 10% against HeLa cells which may be due to the presence of tellurium atom, which was previously reported as anticancer agent [79,80].

4. Conclusions

We can state that much insight has already been gained on the bio-activity of POMs. Here we have adopted a previously used technique to synthesize and encapsulate three different POMs; P_5W_{30}, V_{10} and TeW_6 with CTS to enhance drug carrier properties. The anticancer potential of these synthesized compounds were studied against alkaline phosphatases and Hela cells in a dose-dependent manner to explore their capacity in minimizing side effects through dose adjustment. The anticancer activity of these nanoassemblies, in particular, CTS-P_5W_{30} allows for new strategies of treating cancer. Among the tested compounds, especially CTS-POMs nanoassemblies showed minimum toxicity against normal cells. Our results suggest that the CTS-POMs nanoassemblies have a high potential of treating cancer and its metastasis.

Transparency document

The Transparency document associated with this article can be found in the online version.

References

[1] U. Kortz, A. Müller, J. van Slageren, J. Schnack, N.S. Dalal, M. Dressel, Polyoxometalates: fascinating structures, unique magnetic properties, Coord. Chem. Rev. 253 (2009) 2315–2327.
[2] C.Y. Sun, S.X. Liu, D.D. Liang, K.Z. Shao, Y.H. Ren, Z.M. Su, Highly stable crystalline catalysts based on a microporous metal–organic framework and polyoxometalates, J. Am. Chem. Soc. 131 (2009) 1883–1888.
[3] D.L. Long, R. Tsunashima, L. Cronin, Polyoxometalates: building blocks for functional nanoscale systems, Angew. Chem. Int. Ed. Engl. 49 (2010) 1736–1758.
[4] J.J. Borrás-Almenar, E. Coronado, A. Müller, M.T. Pope, Polyoxometalate Molecular Science, Kluwer Academic Publishers, Dordrecht, The Netherlands, 2003.
[5] M.T. Pope, Y. Jeannin, M. Fournier, Heteropoly and Isopoly Oxometalates, Springer-Verlag, Berlin, 1983.
[6] M.T. Pope, A. Müller, Polyoxometalate chemistry: an old field with new dimensions in several disciplines, Angew. Chem. Int. Ed. Engl. 30 (1991) 34–48.
[7] E.D. Clercq, New anti-HIV agents and targets, Med. Res. Rev. 22 (2002) 531–565.
[8] B. Hasenknopf, Polyoxometalates: introduction to a class of inorganic compounds and their biomedical applications, Front. Biosci. 10 (2005) 275–287.
[9] M. Aureliano, D.C. Crans, Decavanadate, $(V10O28)^{6-}$ and oxovanadates: oxometalates with many biological activities, J. Inorg. Biochem. 103 (2009) 536–546.
[10] H. Stephan, M. Kubeil, F. Emmerling, C.E. Müller, Polyoxometalates as versatile enzyme inhibitors, Eur. J. Inorg. Chem. 2013 (2013) 1585–1594.
[11] J.T. Rhule, C.L. Hill, D.A. Judd, R.F. Schinazi, Polyoxometalates in medicine, Chem. Rev. 98 (1998) 327–358.

[12] P.C. Bruijnincx, P.J. Sadler, New trends for metal complexes with anticancer activity, Curr. Opin. Chem. Biol. 12 (2008) 197–206.
[13] W. Han Ang, P.J. Dyson, Classical and non-classical ruthenium-based anticancer drugs: towards targeted chemotherapy, Eur. J. Inorg. Chem. 2006 (2006) 4003–4018.
[14] F. Noor, A. Wüstholz, R. Kinscherf, N. Metzler-Nolte, A cobaltocenium–peptide bioconjugate shows enhanced cellular uptake and directed nuclear delivery, Angew. Chem. Int. Ed. 44 (2005) 2429–2432.
[15] S.H. van Rijt, P.J. Sadler, Current applications and future potential for bioinorganic chemistry in the development of anticancer drugs, Drug Discov. Today 14 (2009) 1089–1097.
[16] H.L. Seng, E.R. Tiekink, Anticancer potential of selenium and tellurium containing species: opportunities abound!, Appl. Organomet. Chem. 26 (2012) 655.
[17] L. Kelland, The resurgence of platinum-based cancer chemotherapy, Nat. Rev. Cancer 7 (2007) 573–584.
[18] B.W. Harper, A.M. Krause-Heuer, M.P. Grant, M. Manohar, K.B. Garbutcheon-Singh, J.R. Aldrich-Wright, Advances in platinum chemotherapeutics, Chem. Eur. J. 16 (2010) 7064–7077.
[19] A. Ogata, H. Yanagie, E. Ishikawa, Y. Morishita, S. Mitsui, A. Yamashita, K. Hasumi, S. Takamoto, T. Yamase, M. Eriguchi, Antitumour effect of polyoxomolybdates: Induction of apoptotic cell death and autophagy in in vitro and in vivo models, Br. J. Cancer 98 (2008) 399–409.
[20] H. Thomadaki, A. Karaliota, C. Litos, A. Scorilas, Enhanced antileukemic activity of the novel complex 2,5-dihydroxybenzoate molybdenum (VI) against 2,5-dihydroxybenzoate, polyoxometalate of Mo (VI), and tetraphenylphosphonium in the human HL-60 and K562 leukemic cell lines, J. Med. Chem. 50 (2007) 1316–1321.
[21] Z. Dong, R. Tan, J. Cao, Y. Yang, C. Kong, J. Du, S. Zhu, Y. Zhang, J. Lu, B. Huang, Discovery of polyoxometalate-based HDAC inhibitors with profound anticancer activity in vitro and in vivo, Eur. J. Med. Chem. 46 (2011) 2477–2484.
[22] L. Wang, K. Yu, B.B. Zhou, Z.H. Su, S. Gao, L.L. Chu, J.R. Liu, The inhibitory effects of a new cobalt-based polyoxometalate on the growth of human cancer cells, Dalton Trans. 43 (2014) 6070–6078.
[23] F. Zhai, X. Wang, D. Li, H. Zhang, R. Li, L. Song, Synthesis and biological evaluation of decavanadate $Na_4Co(H_2O)_6V_{10}O_{28\cdot18}H_2O$, Biomed. Pharmacother. 63 (2009) 51–55.
[24] L. Wang, B.B. Zhou, K. Yu, Z.H. Su, S. Gao, L.L. Chu, J.R. Liu, G.Y. Yang, Novel antitumor agent, trilacunary keggin-type tungstobismuthate, inhibits proliferation and induces apoptosis in human gastric cancer SGC-7901 Cells, Inorg. Chem. 52 (2013) 5119–5127.
[25] A. Barbera, J. Fernandez-Alvarez, A. Truc, R. Gomis, J. Guinovart, Effects of tungstate in neonatally streptozotocin-induced diabetic rats: mechanism leading to normalization of glycaemia, Diabetologia 40 (1997) 143–149.
[26] M.C. Muñoz, A. Barberà, J. Domínguez, J. Fernàndez-Alvarez, R. Gomis, J.J. Guinovart, Effects of tungstate, a new potential oral antidiabetic agent, in zucker diabetic fatty rats, Diabetes 50 (2001) 131–138.
[27] K. Nomiya, H. Torii, T. Hasegawa, Y. Nemoto, K. Nomura, K. Hashino, M. Uchida, Y. Kato, K. Shimizu, M. Oda, Insulin mimetic effect of a tungstate cluster. Effect of oral administration of homopolyoxotungstates and vanadium-substituted polyoxotungstates on blood glucose level of STZ mice, J. Inorg. Biochem. 86 (2001) 657–667.
[28] A. Barbera, R. Gomis, N. Prats, J. Rodriguez-Gil, M. Domingo, R. Gomis, J. Guinovart, Tungstate is an effective antidiabetic agent in streptozotocin-induced diabetic rats: a long-term study, Diabetologia 44 (2001) 507–513.
[29] J. Rodríguez-Gallardo, R.A. Silvestre, E.M. Egido, J. Marco, Effects of sodium tungstate on insulin and glucagon secretion in the perfused rat pancreas, Eur. J. Pharmacol. 402 (2000) 199–204.
[30] R.A. Silvestre, E.M. Egido, R. Hernández, J. Marco, Tungstate stimulates insulin release and inhibits somatostatin output in the perfused rat pancreas, Eur. J. Pharmacol. 519 (2005) 127–134.
[31] M.M. Gómez-Gómez, N. Rodríguez-Fariñas, B. Cañas-Montalvo, J. Domínguez, J. Guinovart, C. Cámara-Rica, Biospeciation of tungsten in the serum of diabetic and healthy rats treated with the antidiabetic agent sodium tungstate, Talanta 84 (2011) 1011–1018.
[32] G. Fiorani, O. Saoncella, P. Kaner, S. Altinkaya, A. Figoli, M. Bonchio, M. Carraro, Chitosan-polyoxometalate nanocomposites: synthesis, characterization and application as antimicrobial agents, J. Cluster Sci. 25 (2014) 839–854.
[33] M. Inoue, T. Suzuki, Y. Fujita, M. Oda, N. Matsumoto, T. Yamase, Enhancement of antibacterial activity of beta-lactam antibiotics by $[P_2W_{18}O_{62}]6^-$, $[SiMo_{12}O_{40}]^{4-}$, and $[PTi_2W_{10}O_{40}]^{7-}$ against methicillin-resistant and vancomycin-resistant *Staphylococcus aureus*, J. Inorg. Biochem. 100 (2006) 1225–1233.
[34] M. da Silva Coimbra, M. Silva-Carvalho, H. Wisplinghoff, G. Hall, S. Tallent, S. Wallace, M. Edmond, A. Figueiredo, R. Wenzel, Clonal spread of methicillin-resistant *Staphylococcus aureus* in a large geographic area of the United States, J. Hosp. Infect. 53 (2003) 103–110.
[35] D.A. Judd, J.H. Nettles, N. Nevins, J.P. Snyder, D.C. Liotta, J. Tang, J. Ermolieff, R.F. Schinazi, C.L. Hill, Polyoxometalate HIV-1 protease inhibitors. A new mode of protease inhibition, J. Am. Chem. Soc. 123 (2001) 886–897.
[36] K. Dan, T. Yamase, Prevention of the interaction between HVEM, herpes virus entry mediator, and gD, HSV envelope protein, by a Keggin polyoxotungstate, PM-19, Biomed. Pharmacother. 60 (2006) 169–173.
[37] S. Shigeta, S. Mori, E. Kodama, J. Kodama, K. Takahashi, T. Yamase, Broad spectrum anti-RNA virus activities of titanium and vanadium substituted polyoxotungstates, Antiviral Res. 58 (2003) 265–271.
[38] A. Flütsch, T. Schroeder, M.G. Grütter, G.R. Patzke, HIV-1 protease inhibition potential of functionalized polyoxometalates, Bioorg. Med. Chem. Lett. 21 (2011) 1162–1166.
[39] S.G. Mauracher, C. Molitor, R. Al-Oweini, U. Kortz, A. Rompel, Crystallization and preliminary X-ray crystallographic analysis of latent isoform PPO4 mushroom (*Agaricus bisporus*) tyrosinase, Acta Crystallogr. Sect. F: Struct. Biol. Commun. 70 (2014) 263–266.
[40] S.G. Sarafianos, U. Kortz, M.T. Pope, M.J. Modak, Mechanism of polyoxometalate-mediated inactivation of DNA polymerases: an analysis with HIV-1 reverse transcriptase indicates specificity for the DNA-binding cleft, Biochem. J. 319 (1996) 619.
[41] E. Antonova, C. Näther, P. Kögerler, W. Bensch, Organic functionalization of polyoxovanadates: Sb–N bonds and charge control, Angew. Chem. Int. Ed. 50 (2011) 764–767.
[42] Y. Take, Y. Tokutake, Y. Inouye, T. Yoshida, A. Yamamoto, T. Yamase, S. Nakamura, Inhibition of proliferation of human immunodeficiency virus type 1 by novel heteropolyoxotungstates in vitro, Antiviral Res. 15 (1991) 113–124.
[43] A. Ogata, H. Yanagie, E. Ishikawa, Y. Morishita, S. Mitsui, A. Yamashita, K. Hasumi, S. Takamoto, T. Yamase, M. Eriguchi, Antitumour effect of polyoxomolybdates: induction of apoptotic cell death and autophagy in in vitro and in vivo models, Br. J. Cancer 98 (2007) 399–409.
[44] R. Jayakumar, D. Menon, K. Manzoor, S. Nair, H. Tamura, Biomedical applications of chitin and chitosan based nanomaterials—a short review, Carbohydr. Polym. 82 (2010) 227–232.
[45] M. Kumar, R.A. Muzzarelli, C. Muzzarelli, H. Sashiwa, A. Domb, Chitosan chemistry and pharmaceutical perspectives, Chem. Rev. 104 (2004) 6017–6084.
[46] S.F. Peng, M.T. Tseng, Y.C. Ho, M.C. Wei, Z.X. Liao, H.W. Sung, Mechanisms of cellular uptake and intracellular trafficking with chitosan/DNA/poly (γ-glutamic acid) complexes as a gene delivery vector, Biomaterials 32 (2011) 239–248.
[47] Q. Zhao, X. Feng, S. Mei, Z. Jin, Carbon-nanotube-assisted high loading and controlled release of polyoxometalates in biodegradable multilayer thin films, Nanotechnology 20 (2009) 105101.
[48] G. Geisberger, S. Paulus, M. Carraro, M. Bonchio, G.R. Patzke, Synthesis, characterisation and cytotoxicity of polyoxometalate/carboxymethyl chitosan nanocomposites, Chem. Eur. J. 17 (2011) 4619–4625.
[49] T. Meißner, R. Bergmann, J. Oswald, K. Rode, H. Stephan, W. Richter, H. Zänker, W. Kraus, F. Emmerling, G. Reck, Chitosan-encapsulated Keggin anion $[Ti_2W_{10}PO_{40}]^{7-}$. Synthesis, characterization and cellular uptake studies, Transit. Met. Chem. 31 (2006) 603–610.
[50] Y. Feng, Z. Han, J. Peng, J. Lu, B. Xue, L. Li, H. Ma, E. Wang, Fabrication and characterization of multilayer films based on Keggin-type polyoxometalate and chitosan, Mater. Lett. 60 (2006) 1588–1593.
[51] D. Menon, R.T. Thomas, S. Narayanan, S. Maya, R. Jayakumar, F. Hussain, V.K. Lakshmanan, S. Nair, A novel chitosan/polyoxometalate nano-complex for anti-cancer applications, Carbohydr. Polym. 84 (2011) 887–893.
[52] G. Geisberger, E.B. Gyenge, C. Maake, G.R. Patzke, Trimethyl and carboxymethyl chitosan carriers for bio-active polymer-inorganic nanocomposites, Carbohydr. Polym. 91 (2012) 58–67.
[53] L.S. Bergamin, E. Braganhol, R.F. Zanin, M.I. Edelweiss, A.M. Battastini, Ectonucleotidases in tumor cells and tumor-associated immune cells: an overview, J. Biomed. Biotechnol. 2012 (2012) 959848.
[54] C.E. Müller, J. Iqbal, Y. Baqi, H. Zimmermann, A. Röllich, H. Stephan, Polyoxometalates—a new class of potent ecto-nucleoside triphosphate diphosphohydrolase (NTPDase) inhibitors, Bioorg. Med. Chem. Lett. 16 (2006) 5943–5947.
[55] R. Raza, A. Matin, S. Sarwar, M. Barsukova-Stuckart, M. Ibrahim, U. Kortz, J. Iqbal, Polyoxometalates as potent and selective inhibitors of alkaline phosphatases with profound anticancer and amoebicidal activities, Dalton Trans. 41 (2012) 14329–14336.

[56] T.L. Turner, V.H. Nguyen, C.C. McLauchlan, Z. Dymon, B.M. Dorsey, J.D. Hooker, M.A. Jones, Inhibitory effects of decavanadate on several enzymes and *Leishmania tarentolae* in vitro, J. Inorg. Biochem. 108 (2012) 96–104.
[57] K.B. Whitaker, D. Eckland, H. Hodgson, S. Saverymuttu, G. Williams, D. Moss, A variant alkaline phosphatase in renal cell carcinoma, Clin. Chem. 28 (1982) 374–377.
[58] H. Singhal, D.S. Bautista, K.S. Tonkin, F.P. O'Malley, A.B. Tuck, A.F. Chambers, J.F. Harris, Elevated plasma osteopontin in metastatic breast cancer associated with increased tumor burden and decreased survival, Clin. Cancer Res. 3 (1997) 605–611.
[59] A. Berruti, L. Dogliotti, R. Bitossi, G. Fasolis, G. Gorzegno, M. Bellina, M. Torta, F. Porpiglia, D. Fontana, A. Angeli, Incidence of skeletal complications in patients with bone metastatic prostate cancer and hormone refractory disease: predictive role of bone resorption and formation markers evaluated at baseline, J. Urol. 164 (2000) 1248–1253.
[60] R. de Bree, E.E. Deurloo, G.B. Snow, C.R. Leemans, Screening for distant metastases in patients with head and neck cancer, Laryngoscope 110 (2000) 397–401.
[61] G.R. Mundy, Metastasis, Metastasis to bone: causes, consequences and therapeutic opportunities, Nat. Rev. Cancer 2 (2002) 584–593.
[62] J.W. Min, S.W. Um, J.J. Yim, C.G. Yoo, S.K. Han, Y.S. Shim, Y.W. Kim, The role of whole-body FDG PET/CT, Tc 99m MDP bone scintigraphy, and serum alkaline phosphatase in detecting bone metastasis in patients with newly diagnosed lung cancer, J. Korean Med. Sci. 24 (2009) 275–280.
[63] M.H. Alizadeh, S.P. Harmalker, Y. Jeannin, J. Martin-Frere, M.T. Pope, A heteropolyanion with fivefold molecular symmetry that contains a nonlabile encapsulated sodium ion. The structure and chemistry of $[NaP_5W_{30}O_{110}]^{14-}$, J. Am. Chem. Soc. 107 (1985) 2662–2669.
[64] P.J. Domaille, The 1-and 2-dimensional tungsten-183 and vanadium-51 NMR characterization of isopolymetalates and heteropolymetalates, J. Am. Chem. Soc. 106 (1984) 7677–7687.
[65] S. Ramos, R.O. Duarte, J.J. Moura, M. Aureliano, Decavanadate interactions with actin: cysteine oxidation and vanadyl formation, Dalton Trans. (2009) 7985–7994.
[66] K. Schmidt, G. Schrobilgen, J. Sawyer, Hexasodium hexatungstotellurate (VI) 22-hydrate, Acta Crystallogr. Sect. C: Cryst. Struct. Commun. 42 (1986) 1115–1118.
[67] J. Iqbal, An enzyme immobilized microassay in capillary electrophoresis for characterization and inhibition studies of alkaline phosphatases, Anal. Biochem. 414 (2011) 226–231.
[68] H. Van Belle, Alkaline phosphatase. I. Kinetics and inhibition by levamisole of purified isoenzymes from humans, Clin. Chem. 22 (1976) 972–976.
[69] W.H. Fishman, Perspectives on alkaline phosphatase isoenzymes, Am. J. Med. 56 (1974) 617–650.
[70] P. Skehan, R. Storeng, D. Scudiero, A. Monks, J. McMahon, D. Vistica, J.T. Warren, H. Bokesch, S. Kenney, M.R. Boyd, New colorimetric cytotoxicity assay for anticancer-drug screening, J. Natl. Cancer Inst. 82 (1990) 1107–1112.
[71] V. Ball, C. Ringwald, J. Bour, M. Michel, R. Al-Oweini, U. Kortz, Multilayer films made from poly (allylamine) and phosphorous containing polyoxometalates: focus on the zeta potential, J. Colloid Interface Sci. 409 (2013) 166–173.
[72] R.M. Glickman, D.H. Alpers, G.D. Drummey, K.J. Isselbacher, Increased lymph alkaline phosphatase after fat feeding: effects of medium chain triglycerides and inhibition of protein synthesis, Biochim. Biophys. Acta 201 (1970) 226–235.
[73] K.B. Whitaker, D. Eckland, H.J. Hodgson, S. Saverymuttu, G. Williams, D.W. Moss, A variant alkaline phosphatase in renal cell carcinoma, Clin. Chem. 28 (1982) 374–377.
[74] R.H. Glew, M.S. Czuczman, W.F. Diven, R.L. Berens, M.T. Pope, D.E. Katsoulis, Partial purification and characterization of particulate acid phosphatase of *Leishmania donovani* promastigotes, Comp. Biochem. Physiol. B 72 (1982) 581–590.
[75] M. Halperin-Sheinfeld, A. Gertler, E. Okun, B. Sredni, H.Y. Cohen, The Tellurium compound, AS101, increases SIRT1 level and activity and prevents type 2 diabetes, Aging (Milano) 4 (2012) 436.
[76] K.S. Soppimath, T.M. Aminabhavi, A.R. Kulkarni, W.E. Rudzinski, Biodegradable polymeric nanoparticles as drug delivery devices, J. Controlled Release 70 (2001) 1–20.
[77] D. Rehder, The future of/for vanadium, Dalton Trans. 42 (2013) 11749–11761.
[78] G. Fraqueza, C.A. Ohlin, W.H. Casey, M. Aureliano, Sarcoplasmic reticulum calcium ATPase interactions with decaniobate, decavanadate, vanadate, tungstate and molybdate, J. Inorg. Biochem. 107 (2012) 82–89.
[79] R.L. Cunha, I.E. Gouvea, L. Juliano, A glimpse on biological activities of tellurium compounds, An. Acad. Bras. Cienc. 81 (2009) 393–407.
[80] B. Sredni, Immunomodulating tellurium compounds as anti-cancer agents, Semin. Cancer Biol. 6 (2012) 0–69.